Angle-resolved photoemission investigation of the electronic band properties of $YBa_2Cu_3O_{7-x}$ (001)

Y. Sakisaka, T. Komeda, T. Maruyama, and M. Onchi
Department of Chemistry, Faculty of Science, Kyoto University, Kyoto 606, Japan

H. Kato
Photon Factory, National Laboratory for High Energy Physics, Tsukuba-shi, Ibaraki 305, Japan

Y. Aiura and H. Yanashima
Institute of Physics, University of Tsukuba, Tsukuba-shi, Ibaraki 305, Japan

T. Terashima and Y. Bando
Institute for Chemical Research, Kyoto University, Uji 611, Japan

K. Iijima, K. Yamamoto, and K. Hirata
Research Institute for Production Development, Kyoto 606, Japan
(Received 21 October 1988; revised manuscript received 19 December 1988)

The electronic energy-band properties of epitaxially grown $YBa_2Cu_3O_{7-x}$(001) single-crystal thin films have been investigated by angle-resolved ultraviolet photoemission spectroscopy (ARUPS) with synchrotron radiation as the light source. The (001) surfaces exhibit sharp (1×1) low-energy electron-diffraction patterns. Our ARUPS data show a clear Fermi edge and dispersive nature of the valence bands, suggesting the validity of the band concept for this oxide. We determined energy-band dispersion along the Γ-*X*-*M*-Γ directions in the bulk Brillouin zone. The experimental results are compared with the existing ground-state band calculations.

I. INTRODUCTION

The discovery of the superconductor $YBa_2Cu_3O_{7-x}$ (hereafter referred to as Y-Ba-Cu-O) with a critical temperature (T_c) of ~90 K,[1] far above that previously considered possible for superconductivity, has stimulated intense investigation of the superconducting mechanisms and properties of this material. However, there is no agreement to date on why the T_c of this superconductor is so high.

The traditional Bardeen-Cooper-Schrieffer (BCS) theory[2] predicts T_c of only 30–40 K. The key assumptions of the BCS theory are that the electron-phonon coupling responsible for electron pairing is weak and that the band picture based on the one-electron approximation is valid for the normal-state electronic structure, i.e., a sharp Fermi surface exists. Thus, the observed high T_c and the lack of an isotope effect[3] in Y-Ba-Cu-O have case doubt on the weak-coupling approximation as well as the validity of the band picture in Y-Ba-Cu-O, suggesting that on-site electron-electron correlation effects play a dominant role and break the one-electron picture. This is the point of this story.

Whether or not the band picture is valid in this oxide is a vital key factor concerned with the essence of the superconducting mechanism.

Several angle-integrated ultraviolet photoemission spectroscopy (AIUPS) experiments on sintered pellets of this oxide[4–15] have been made to explore the angle-integrated density of occupied states and show the disagreement between observed and calculated spectra[16–22] and the existence of a valence-band satellite. These AIUPS studies concluded the strong electron correlations and therefore the breakdown of the band picture. However, a major problem in the study of sintered materials is the quality of the sample. Scraping with a diamond file to prepare a fresh surface may destroy the compound selvage.[23] It is known that oxygen is easily released from the surface into the vacuum by scraping[4,24,25] and also by cleaving.[26] Furthermore, angle integration smears fine structures near the Fermi energy (E_F). Angle-resolved photoemission spectroscopy (ARUPS) and sufficiently large single crystals should be used to test the details of the band structure close to E_F.

Recently, Stoffel *et al.*[27] reported an ARUPS study of cleaved single-crystal samples and claimed that the leading edge near E_F showed dispersion. Unfortunately, they found no clear Fermi edge, however.

It will be shown below that the quality of the sample surface plays a crucial role in obtaining spectra with features sharp enough to identify the states near E_F.

Note that electron correlations are already strong in any ordinary metal. At this point, one interesting observation should be mentioned. Very recently, Hoffmann *et al.*[28] studied the Fermi surface of Y-Ba-Cu-O by positron annihilation and found good correlation with the calculated band structure of Refs. 17 and 18. Naturally, questions arise as to whether or not the electronic structure is determined by unusually strong electron correlations and, therefore, incompatible with the band picture, though we admit the observed peak positions may shift from the corresponding peak in the band-structure calculations. Accurate and precise ARUPS measurements on carefully characterized specimens are highly desired for the correct

electronic structure to be clarified. We recently reported preliminary ARUPS results for Y-Ba-Cu-O(001),[29] where we found some photoemission features which favor a one-electron band picture rather than a localized one, contrary to the previous studies on the sintered samples.[4-15]

In this paper, we present a detailed ARUPS study of high-quality epitaxial Y-Ba-Cu-O(001) films at 300 K to elucidate the normal-state electronic structures. An understanding of the normal state is a vital first step for determining the superconducting mechanism. As mentioned below, the samples used displayed sharp (1×1) low-energy electron-diffraction (LEED) patterns and their superconducting properties were found to be kept at 300 K even in vacuum for at least 1-2 weeks. Our ARUPS data show a clear Fermi edge, fine structures near E_F, and dispersion effects on the valence bands of this oxide compatible with the band picture. The experimental results are compared with the existing band calculations.[16-22]

II. EXPERIMENT

The ARUPS experiments were done at the Photon Factory as described elsewhere.[30] The angular resolution was ±1° and the total energy resolution was ~0.1-0.2 eV depending on the photon energies ($h\nu$) of 23-80 eV. Baking of the ARUPS chamber was done at ~80-100 °C for ~50 h to prevent loss of oxygen from the sample.[31] The base pressure in the system was 2×10^{-10} Torr. A Pt foil in electrical contact with the samples provided the Fermi-level reference of the photoemission spectra. Throughout the whole experiment, the surface component of the vector potential (A) of the incident light was in the [100](ΓX) direction ($A_\parallel$ along [100]).

All the measurements were made at 300 K and on two separate samples (Nos. 1 and 2) of single-crystal Y-Ba-Cu-O films (~10 mm diam×1000 Å thick) which were prepared epitaxially on $SrTiO_3$(001) substrates as described in Ref. 32. Identical data were obtained from both samples, and therefore, the sample number will not be referred hereafter, unless necessary. The sample was mounted flat to a 0.5-mm-thick Pt sheet spot welded to a Pt heater assembly and was held securely with Pt tabs. The temperature was measured by a chromel-alumel thermocouple spot welded to the tab.

In the ARUPS chamber, the samples were annealed at ~600 °C for ~20 min in ~100 Torr O_2 and then cooled to room temperature very slowly, keeping the oxygen atmosphere. After this oxygen treatment and the subsequent evacuation of the chamber, the system pressure in the low-10^{-9} Torr range was achieved. The cleanness of the surfaces was confirmed by Auger electron spectroscopy (AES) and their crystalline order by LEED. To avoid possible surface damage, AES and LEED were employed only after ARUPS measurements were completed on a given sample. As a matter of fact, we found no changes with time in the AES spectra and the LEED patterns of samples under electron irradiation over ~1 h, in contrast to the earlier findings on the sintered samples.[10] Finally, several days after, the superconducting transition was checked and the endpoint of dc-resistive transition [$T_c(R=0)$] occurred at 88 K with a transition width ΔT (10%-90%) of ~1.5 K (the resistivity at 290 K was ~200 $\mu\Omega$ cm) as before. Thus, our samples are stable in vacuum even at room temperature for at least 1-2 weeks, being contrary to the sintered ones. That is, earlier studies on the sintered samples by other groups[4] showed that oxygen leaves the scraped surface in vacuum, even at room temperature and that oxygen deficiency sensitively reduces the T_c values.

The work function of the sample was determined by using the secondary electron threshold in photoemission. We obtained the work function $\Phi=5.1$ eV.

III. RESULTS AND DISCUSSION

A. AES and LEED

Figure 1(a) shows a typical Auger spectrum [$dN(E)/dE$] of Y-Ba-Cu-O(001) measured at a primary electron energy of $E_p=2$ keV. Yttrium (Y), barium (Ba), copper (Cu), and oxygen (O) peaks are observed as indicated in

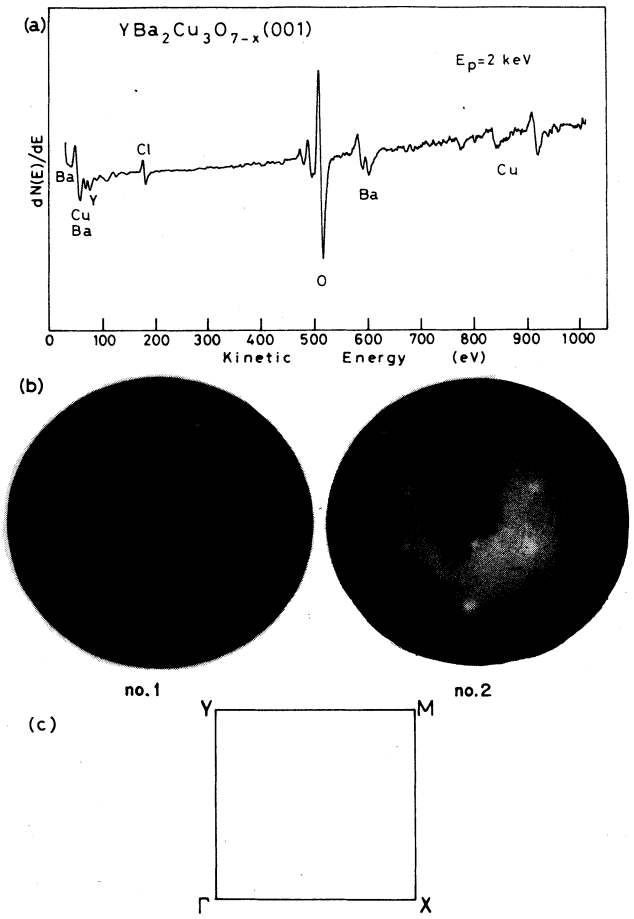

FIG. 1. (a) Typical Auger spectrum of $YBa_2Cu_3O_{7-x}$ (001) ($E_p=2$ keV). (b) LEED patterns for $YBa_2Cu_3O_{7-x}$ (001), No. 1 ($E_p=74$ eV) [left] and No. 2 ($E_p=68$ eV) [right]. (c) ΓXMY[(001)] plane of the Brillouin zone.

the figure. Note that our samples are free from carbon (C) contamination. Instead, a small chlorine (Cl) peak at ~180 eV is detected as seen in Fig. 1(a). Using elemental sensitivity factors, the Cl concentration was roughly estimated to be ~6% of the Cu concentration. The Cl peak intensity varies somewhat from sample to sample. However, we were not able to identify any contribution from this chlorine to the valence-band ARUPS spectra. In other words, the ARUPS spectra are unaffected by Cl at this level.

From the AES results, the Auger-peak intensity ratio $I[0(KLL,510\text{ eV})]/I[\text{Cu}(LVV,920\text{ eV})]$ was found to be ~4.6 for our Y-Ba-Cu-O samples. Using the same ratio $I(\text{O})/I(\text{Cu})$ of ~2.0 for CuO,[33] the ratio of the atomic concentrations for O and Cu in the Y-Ba-Cu-O samples used is roughly estimated to be ~2.3. In other words, these results indicate that the oxygen-deficiency value x in the chemical formula $YBa_2Cu_3O_{7-x}$ is ~0.1 for our samples as expected (i.e., $YBa_2Cu_3O_{6.9}$).

The LEED patterns at $E_p=60$–100 eV showed sharp spots which have the (1×1) symmetry and reflect the nearly square two-dimensional (2D) Brillouin zone (BZ) of the (001) face [see Fig. 1(c) for BZ]. Figure 1(b) shows examples of LEED patterns for samples No. 1 (left) and No. 2 (right). As illustrated in the figure, the pattern for sample No. 1 has a sufficiently low background, while that for sample No. 2 has a slightly bright background which looks comparable to the case of Ref. 27. Such a bright background can be considered the coexistence of poorly ordered small domains, which might cause density-of-states features in the ARUPS spectra. However, in spite of this fear, as shown below, we found that the ARUPS spectra of sample No. 2 exhibit the same angular dependence as those of sample No. 1, with an exception of a feature at ~8.5 eV below E_F.

B. ARUPS

For Y-Ba-Cu-O a number of state-of-the-art band-structure calculations are available[16–22] and indicate that the valence bands are indeed dominated by strongly hybridized overlapping Cu $3d$ and O $2p$ states. The calculated band structures are similar to one another except for the details. As an example, the calculated band structure of Y-Ba-Cu-O by Massidda *et al.*[17] is shown in Fig. 2 (we maintain the same symmetry labels as in Refs. 16 and 29). The valence-band structure comes from a complex set of 36 bands and, therefore, it is impossible to observe each band separately even by ARUPS. However, we note rather simple band structures near the top (E_F) and bottom and a large band gap (or an area of low density of states) at ~2–3 eV below E_F at M (indicated by shaded regions in Fig. 2). It seems that such structures can be identified by ARUPS.

Figure 3 shows the $h\nu$ dependence of the normal-emission spectra of the Y-Ba-Cu-O(001) samples measured at a light incidence angle of $\theta_i=60°$ from the surface normal: (a) sample No. 1 for $h\nu=25$–60 eV (from Ref. 29) and (b) sample No. 2 for $h\nu=70$–80 eV near the Cu $3p$ resonance. The binding energy (E_b) is given with respect to E_F. Emission from states near E_F (see below) is very small, being consistent with band-structure calculations.[16–18] In the low-E_b region between E_F and ~10 eV, four major features are seen at ~3, ~5, ~7, and ~8.5 eV, which do not move within ±0.2 eV with $h\nu$ in agreement with the highly 2D nature of the band structure (see Fig. 2). Note that each feature does not correspond to a single band but to a group of bands. In addition, as reported earlier,[5,8,10,14,15] the Ba $5p$ doublet peaks at 13.2 and 15.3 eV and a resonating-valence-band satellite feature (S) at ~12.5 eV are observed [see Fig. 3(b)]. The positions of the Ba $5p$ doublet were determined by using the $h\nu=105$ eV spectrum where the Ba states are enhanced by the Ba $4d\rightarrow 4f$ resonance.

In Fig. 3(a) for sample No. 1, the 8.5-eV feature is seen only at $h\nu\sim40$ eV and, therefore, is considered to be due to an umklapp process involving the reciprocal-lattice vector G(110), in contrast to a feature previously observed at 9–10 eV in the spectra of the sintered materials[5,8–15] and in Refs. 27, 34, and 35. The 9–10 eV feature, which has been attributed to contamination by carbonates[9] or wa-

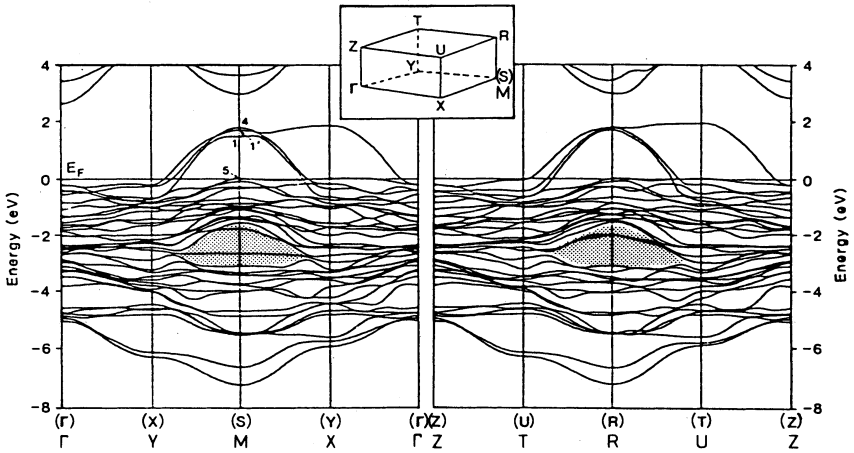

FIG. 2. Energy bands of $YBa_2Cu_3O_7$ calculated by Massidda *et al.* (from Ref. 17). The symmetry labels used in Ref. 17 are given in parentheses.

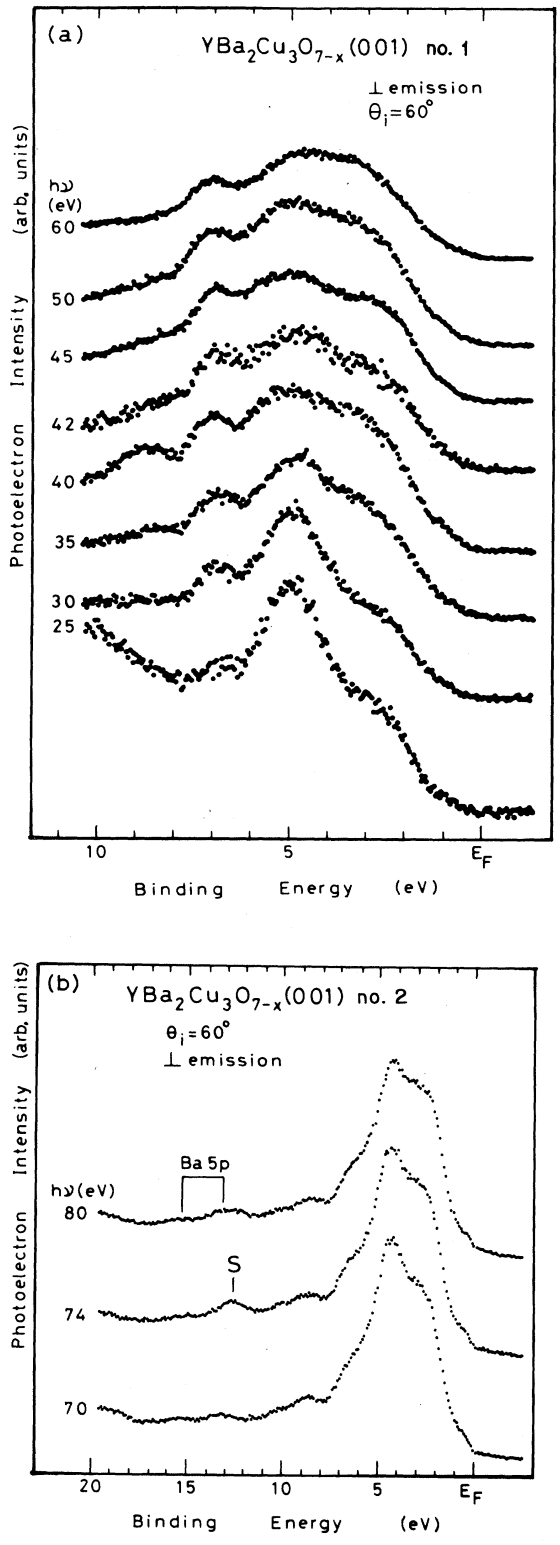

FIG. 3. (a) $h\nu$ dependence of normal-emission spectra of $YBa_2Cu_3O_{7-x}$ (001), No. 1, measured at $\theta_i = 60°$ ($25 \leqq h\nu \leqq 60$ eV) (from Ref. 29). (b) Normal-emission spectra of $YBa_2Cu_3O_{7-x}$(001), No. 2, measured at $\theta_i = 60°$ and $70 \leqq h\nu \leqq 80$ eV near the Cu $3p$ resonance.

ter,[14] becomes weak with increasing $h\nu$ from 25 to 180 eV.[5,8-10,14,34,35] Very recently, Wendin[36] explained the 9–10 eV feature as a two-hole satellite of a primarily oxygen-related state at ~3 eV (see also Refs. 15, 34, and 35). In the case of the sintered samples, a portion of this 9.5-eV feature is likely to be due to contamination. However, our findings flatly contradict the Wendin's explanation (see Ref. 36). We propose that this feature in the AIUPS spectra is a density-of-states structure and reflects high density of states regions near M, i.e., the bottom band (see below). This proposal may be supported by the data for sample No. 2 in Fig. 3(b), where the weak ~9 eV feature exists for all $h\nu$ used. As stated above (Sec. III A), the LEED results show the existence of a small quantity of poorly ordered domains for sample No. 2. With an exception of this 8.5-eV feature, identical AR-UPS spectra were obtained from both samples, however.

As seen in Figs. 3(a) and 3(b), with increasing $h\nu$ from 25 to 80 eV, the intensity of the 3-eV feature becomes strong relative to that of the 5-eV feature, in contrast to the results previously obtained on the sintered samples.[4,10] Examination of photoionization cross section tables[37] indicates that the ratio of atomic Cu $3d$ and O $2p$ cross sections increases at higher $h\nu$. Thus, our observations suggest that the Cu $3d$ states are more heavily involved in the bands near 3 eV than in those near 5 eV, though, in the

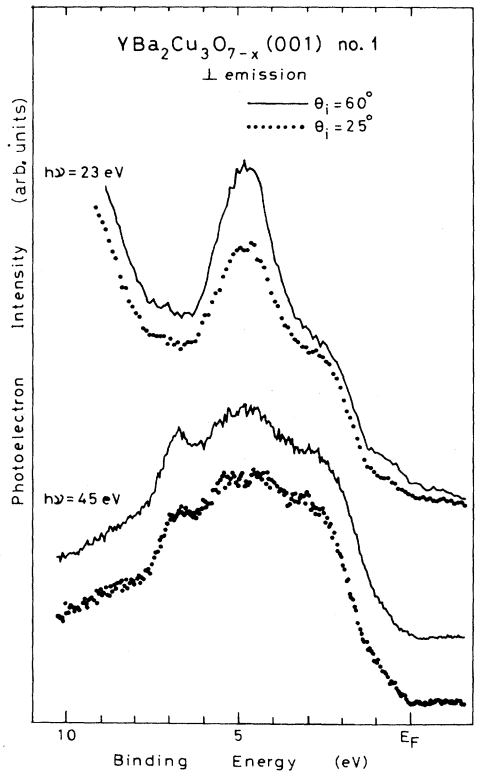

FIG. 4. θ_i dependence of normal-emission spectra of $YBa_2Cu_3O_{7-x}$ (001), No. 1, for binding energies between E_F and ~2 eV measured at $h\nu = 23$ and 45 eV: $\theta_i = 25°$ (dots) and $\theta_i = 60°$ (lines).

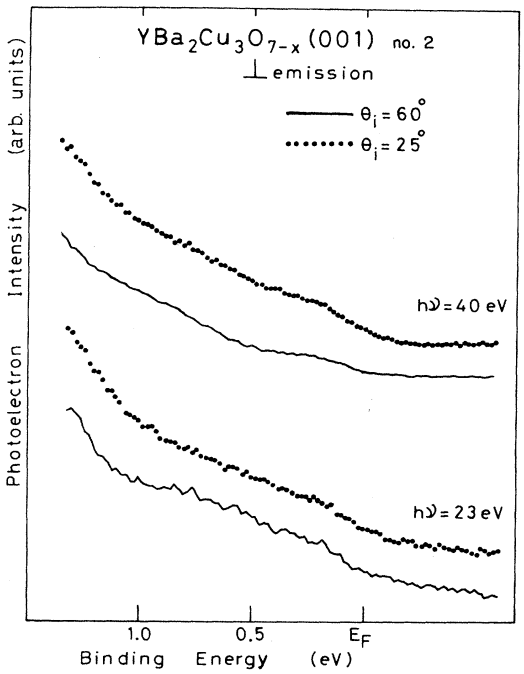

FIG. 5. Details of normal-emission spectra of $YBa_2Cu_3O_{7-x}$ (001), No. 2, in the Fermi-edge region measured at $h\nu=23$ and 40 eV: $\theta_i=25°$ (dots) and $\theta_i=60°$ (lines).

strict sense, the distortion of the valence-electron wave functions in the solid environment with respect to the atomic case and the diffraction effects on the intensity profiles should be properly taken into account.

Figure 4 shows the normal-emission spectra of Y-Ba-Cu-O(001) measured at both $\theta_i=60°$ (lines) and 25° (dots) for $h\nu=23$ and 45 eV. We note that the 5-eV feature, and maybe the 7-eV feature also, is stronger for $\theta_i=60°$. Furthermore, the structure between E_F and ~ 1 eV is also stronger for $\theta_i=60°$ as clearly seen in the $h\nu=23$ eV spectra. These results lead to the conclusion that there are more Δ_1-symmetry bands in the energy regions near E_F, ~ 5, and ~ 7 eV than in the other regions. The normal-emission spectra of Y-Ba-Cu-O(001) in the low-E_b region between E_F and ~ 1 eV are shown in more detail in Fig. 5 [measured at $\theta_i=60°$ (lines) and 25° (dots) both for $h\nu=23$ and 40 eV]. Roughly speaking, two major features exist at ~ 0.25 and ~ 0.75 eV (see below for further details): the former (the latter) is more clearly seen in the $h\nu=40$ (30) eV spectra. Although the θ_i dependence is marginal, the feature at ~ 0.75 eV in the $h\nu=23$ eV spectra looks stronger for $\theta_i=60°$, suggesting that the bands at ~ 0.75 eV contains much contributions from O $2p$ states of Δ_1 symmetry. Note that this does not necessarily rebut the earlier suggestion[13] that there are Cu $3d$ contributions to the states very near E_F. Later (Sec. III C), we show that these fine structures disappear

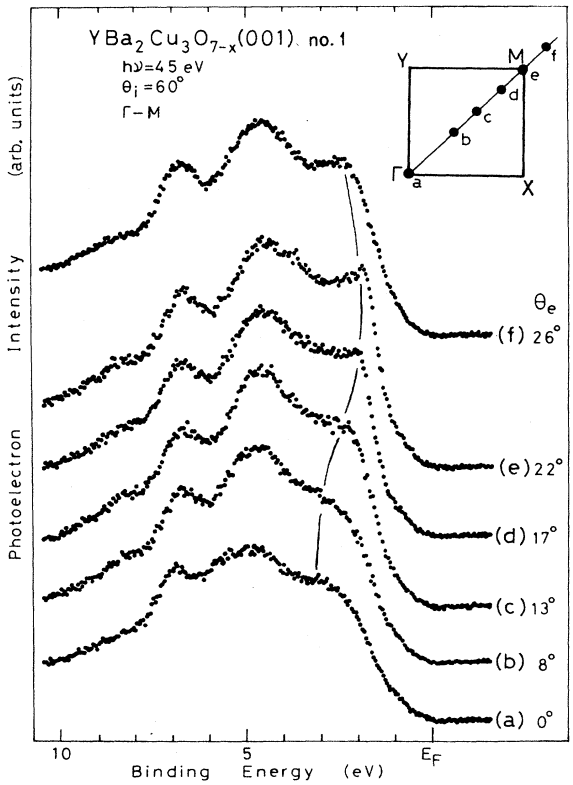

FIG. 6. Angle-resolved photoemission spectra of $YBa_2Cu_3O_{7-x}$ (001), No. 1, along Γ-M measured at $h\nu=45$ eV and $\theta_i=60°$ (from Ref. 29).

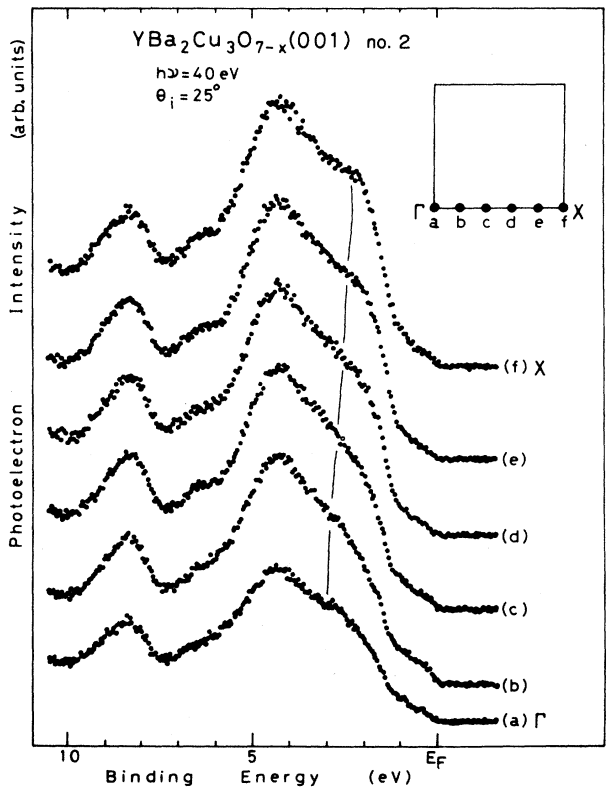

FIG. 7. Angle-resolved photoemission spectra of $YBa_2Cu_3O_{7-x}$ (001), No. 2, along Γ-X measured at $h\nu=40$ eV and $\theta_i=25°$.

after heating the sample in vacuum.

Figure 6 shows off-normal spectra of Y-Ba-Cu-O(001) taken at $h\nu=45$ eV and $\theta_i=60°$ along Γ-M (from Ref. 29). The average position in k space (BZ) where each spectrum probes is also indicated in each figure. The 5- and 7-eV features stay at almost fixed locations as k is changed, while the 3-eV feature at $k=0$ (Γ) disperses to lower binding energy with increasing k from Γ to M ($\sim$2 eV at M) and thereafter to higher binding energy. We found that at Γ in the second zone the spectrum returns to that at Γ in the first zone and that along Γ-M-Γ the dispersion of the 3-eV feature is periodic about the M point (see Fig. 3 of Ref. 29). Similar results were also obtained for $h\nu=40$ and 50 eV (not shown). Thus, the dispersion of the 3-eV feature exhibits the correct periodicity for the (1×1) structure. A large valley at $\sim$3 eV seen in the spectra at M can be considered to reflect the large band gap (or the area of low density of states) in the range $\sim$2 to $\sim$3.5 eV at around M in the calculated band structure of Refs. 17 (shaded regions in Fig. 2), 19, and 20. The band calculations of Ref. 17 (Fig. 2) shows that the upper main bands in the first $\sim$1 eV above the "band gap" (shaded regions in Fig. 2) exhibit relatively large dispersion ($\sim$1.4-eV dispersion) along Γ-M as compared with the lower ones ($\sim$0.6-eV dispersion) in the first $\sim$1 eV below the "band gap" (see also Ref. 19), in accord with our observations. Furthermore, the band calculation of Ref. 17 predicts the nearly dispersionless bands at $\sim$2 eV below the bottom of the "band gap" (i.e., at $\sim$5 eV below E_F). Regardless of a discrepancy of $\sim$2 eV, we associate the observed 7-eV feature with such bands (see below).

As seen in Fig. 6, the 8.5-eV feature is visible away from Γ and most pronounced at around M. This feature appears to disperse from $\sim$7.5 eV at Γ to $\sim$8.5 eV at M. However, we cannot decide firmly from the present data whether this result is related to real dispersion effect or simply to varying peak intensity. Only the band calculation of Ref. 21 predicts the bottom band at $\sim$8.5 eV at M in agreement with our results, but its band structure in the Fermi-edge region is very different from the other calculations of Refs. 16–20 and 22 and also disagrees with our data (see below). The measured positions of the "gap" and peaks do not agree with any band calculation (except for Ref. 21). The energy shift required for agreement is $\sim$1 eV as an average, as suggested earlier.[4,13] However,

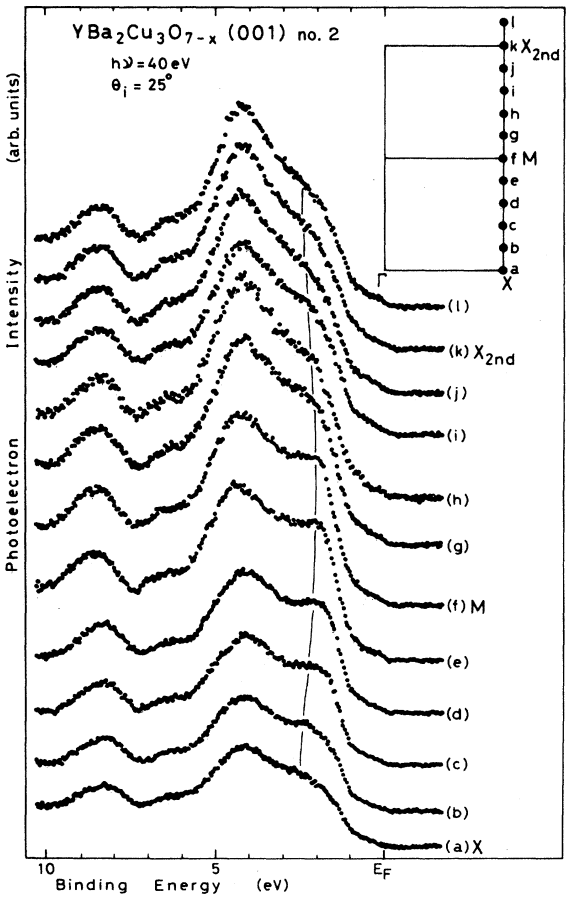

FIG. 8. Angle-resolved photoemission spectra of $YBa_2Cu_3O_{7-x}$ (001), No. 2, along X-M-X measured at $h\nu=40$ eV and $\theta_i=25°$.

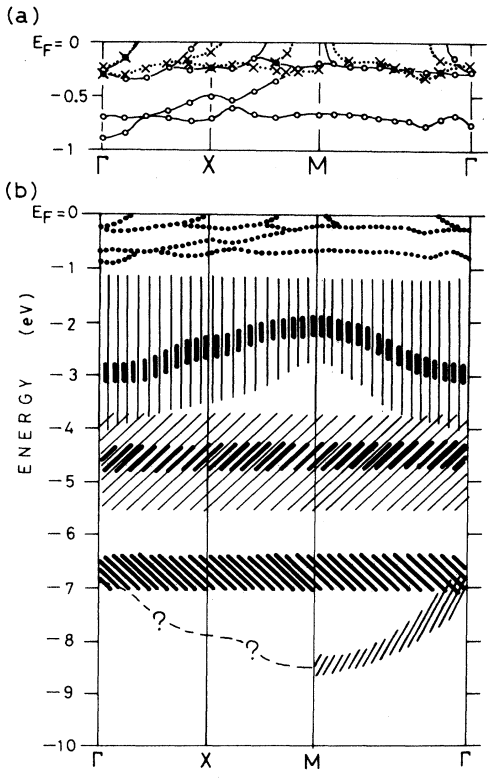

FIG. 9. (a) Binding energies of the fine structures in the Fermi-edge region as a function of the wave vector **k** along Γ-X-M-Γ. The crosses (×) connected by dotted lines are data points derived from Fig. 10(a). The open circles (○) connected by solid lines are data points derived from Fig. 10(b). (b) Experimentally determined schematic band structure of $YBa_2Cu_3O_{7-x}$.

we note that the correspondence between experiment and calculation is fairly improved when the calculated band width in Refs. 16, 17, 19, and 20 is expanded by 20–30%.

Figures 7 and 8 show off-normal spectra of Y-Ba-Cu-O(001) taken at $h\nu=40$ eV and $\theta_i=25°$ along Γ-X and X-M-X, respectively. The same argument as described above for the data along Γ-M can be held for these data along Γ-X and X-M. Therefore, we do not repeat it again, except for a few comments of particular relevance to the data in Figs. 7 and 8. The feature at -3 eV at $k=0$ (Γ) shows relatively small dispersion of ~ 0.5 eV along Γ-X and X-M: this feature disperses from ~ 3 eV at Γ to ~ 2.5 eV at X, and then to ~ 2 eV at M (the thin solid line in each figure is only intended as an aid to the eye and represents the possible dispersion of this feature). Such small dispersion along Γ-X and X-M is consistent with the band calculations of Refs. 17 (Fig. 2) and 19. Figure 8 shows that along X-M-X the dispersion of this feature is periodic about the M point, leading to the same conclusion as above that the dispersion exhibits the correct periodici-

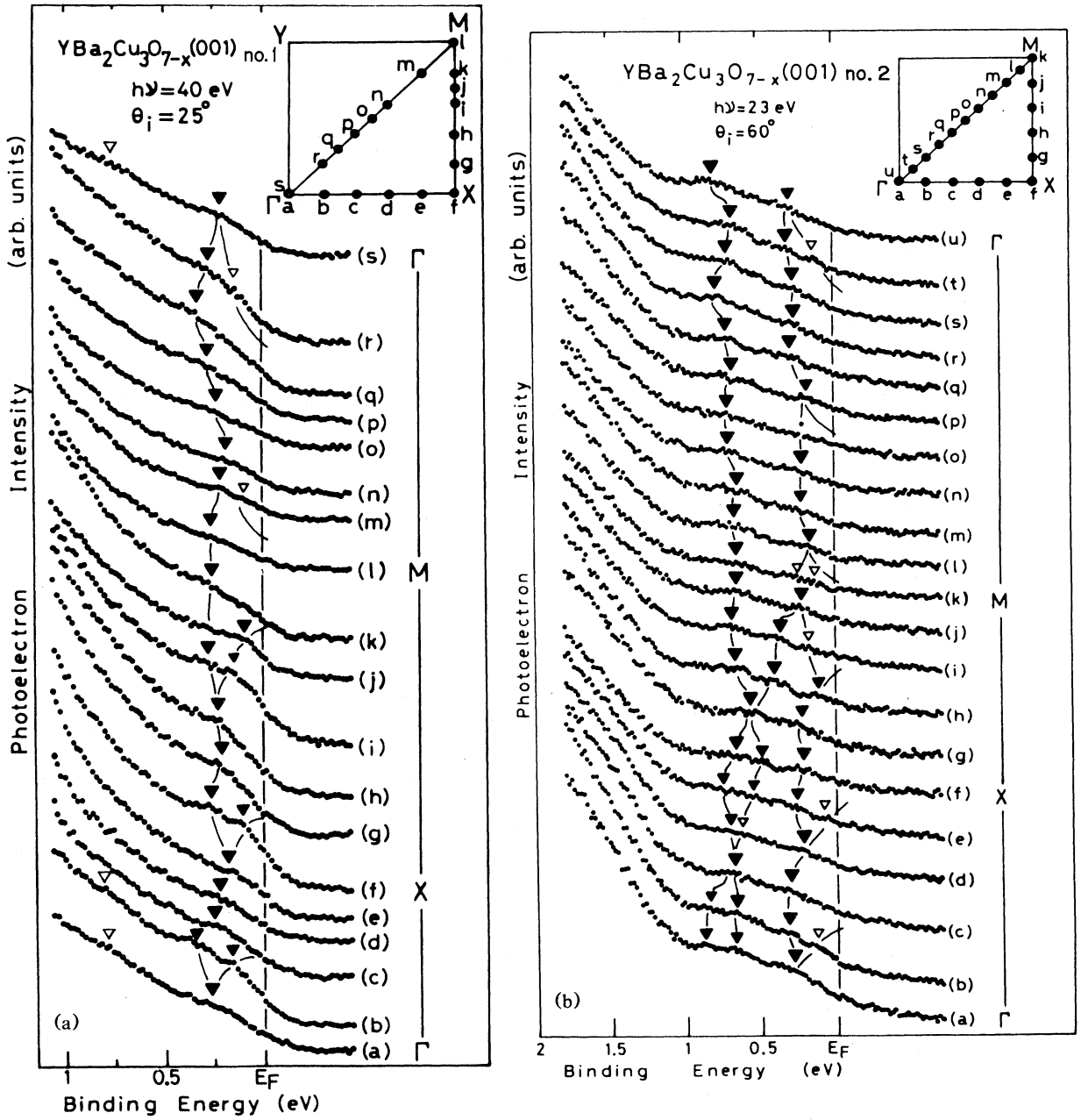

FIG. 10. (a) Angle-resolved photoemission spectra of $YBa_2Cu_3O_{7-x}$ (001), No. 1, in the Fermi-edge region along Γ-X-M-Γ measured at $h\nu=40$ eV and $\theta_i=25°$ (from Ref. 29). (b) Angle-resolved photoemission spectra of $YBa_2Cu_3O_{7-x}$ (001), No. 2, in the Fermi-edge region along Γ-X-M-Γ measured at $h\nu=23$ eV and $\theta_i=60°$ (from Ref. 29).

ty for the (1×1) structure. Unfortunately, the accidental appearance of the 8.5-eV feature at $h\nu=40$ eV (see above) prevents us from observing the dispersion of the bottom bands in Figs. 7 and 8.

We want to stress that the calculation of the k-resolved density of states including the optical matrix elements is highly desired for a direct comparison between observed and calculated ones.

To summarize, the schematic band structure of Y-Ba-Cu-O for $1\leqq E_b\leqq 8.5$ eV which is derived from our ARUPS data is shown in Fig. 9(b). Compare it to the calculated band structure of Ref. 17 (Fig. 2). As for the band structure between E_F and ~1 eV, we will discuss that below.

As has been reported in Ref. 29, the dispersive nature of the valence bands is also seen for the states near E_F. More importantly, a clear Fermi edge is observed.[38] For completeness, we reproduce the data in Figs. 10(a) and 10(b) (from Ref. 29), which are off-normal spectra in the Fermi-edge region along Γ-X-M-Γ measured at $h\nu=40$ eV and $\theta_i=25°$ and measured at $h\nu=23$ eV and $\theta_i=60°$, respectively. The average position in k space (BZ) where each spectrum probes is indicated in each figure. Each of the fine structures observed in Fig. 10(a) has a counterpart in Fig. 10(b).[39] The clear Fermi edge is seen in spectra (f), (i), and (j) in Fig. 10(a), i.e., only at specific k points. Note that the fine structures disperse with k and some of them look to cross E_F as tentatively indicated by thin solid lines in each figure. The measured dispersion of the fine structures is plotted in Fig. 9(a) as a function of $k_\parallel$ in the BZ of 2D character. The crosses ($\times$) connected by dotted lines are experimental points measured at

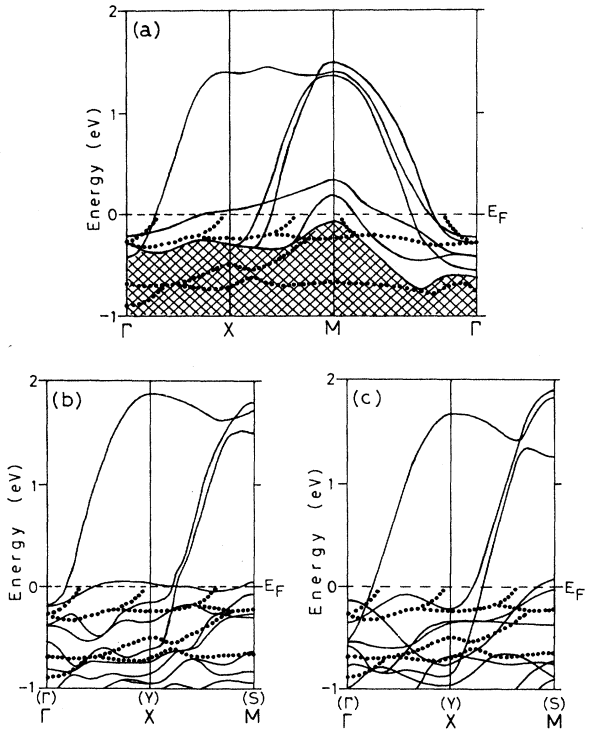

FIG. 11. Comparison of experimental and theoretical band structure of $YBa_2Cu_3O_{7-x}$ in the Fermi-edge region along Γ-X-M-Γ. The dotted lines represent the experimental bands shown in Fig. 9(b). The solid lines represent the calculated bands of (a) Mattheiss and Hamann (from Ref. 16), (b) Yu *et al.* (from Ref. 18), and (c) Xu *et al.* (from Ref. 22). The symmetry labels used in Refs. 18 and 22 are given in parentheses.

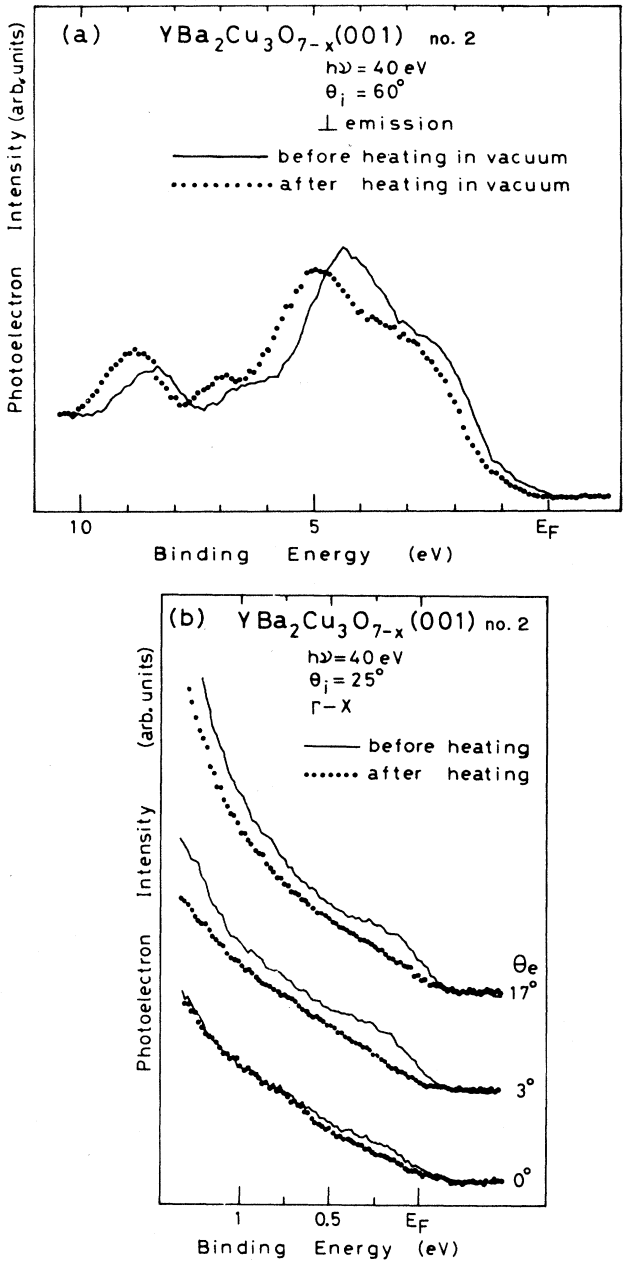

FIG. 12. (a) Normal-emission spectra of $YBa_2Cu_3O_{7-x}$ (001), No. 2, for binding energies between E_F and ~10 eV measured before (line) and after (dots) heating at $\sim600\,°C$ in vacuum ($h\nu=40$ eV and $\theta_i=60°$). (b) Angle-resolved photoemission spectra of $YBa_2Cu_3O_{7-x}$(001), No. 2, in the Fermi-edge region at various θ_e along Γ-X before (lines) and after (dots) heating at $\sim600\,°C$ in vacuum ($h\nu=40$ eV and $\theta_i=25°$).

$h\nu=40$ eV [Fig. 10(a)], while the open circles (○) connected by solid lines are experimental points measured at $h\nu=23$ eV [Fig. 10(b)]. The experimental band structure between E_F and ~ 1 eV obtained by averaging the two sets of data is shown by dotted lines in Fig. 9(b).

In order to compare our experimental band structure in the Fermi edge region with the state-of-the-art band structure calculations for Y-Ba-Cu-O, we plot the experimental bands in Fig. 9(b) (dotted lines) over the calculated band structures (solid lines) of Mattheiss and Hamann (Ref. 16), Yu *et al.* (Ref. 18), and Xu *et al.* (Ref. 22) in Figs. 11(a), 11(b), and 11(c), respectively. Although the complexity of the calculated bands below E_F makes it hard to compare with the observation, there is some resemblance between them. For example, the experimental bands cross E_F near Γ along Γ-X, near X, in the midpoint between X and M, near M, and near Γ along M-Γ, which is consistent with the calculations. As for the bands between ~ 0.4 and ~ 1 eV, see Figs. 11(b) and 11(c). However, at present, we hesitate to decide which band calculation to choose.

C. Effect of heating in vacuum

Separate experiments in our laboratory showed that the LEED pattern was apparently unchanged during the crystal heating up to ~ 400 °C in vacuum. However, beyond ~ 400 °C, the LEED spots became weak accompanied with a background increase and then disappeared at ~ 450 °C. From the dc-resistive measurements, it was found that after vacuum heating to ~ 400 °C the Y-Ba-Cu-O(001) films showed no superconductivity but characteristic semiconducting behaviors.

Figure 12(a) shows normal-emission spectra of Y-Ba-Cu-O(001) in the energy region between E_F and ~ 10 eV, measured before and after heating at ~ 600 °C in vacuum for ~ 15 min ($h\nu=40$ eV and $\theta_i=60°$). Figure 12(b) shows the details of ARUPS spectra in the Fermi-edge region at various emission angles (θ_e) along Γ-X for the same sample before and after the same heat treatment ($h\nu=40$ eV and $\theta_i=25°$). It is well known that such a vacuum heating leads to a loss of oxygen from the surface.[40] As seen in the figures, by this heating, the features closest to E_F are reduced, while the spectral features between ~ 1 and ~ 10 eV are unchanged except for a uniform shift by ~ 1 eV towards higher binding energy and a slight reduction of the feature at ~ 5 eV. We associate this decrease of the 5-eV feature with oxygen leaving the surface. Since oxygen vacancies may act as donors, the relative upward shift of E_F is expected with the removal of oxygen. These findings indicate that the observed near-edge states are characteristic of the superconductor.

IV. SUMMARY AND CONCLUDING REMARKS

ARUPS experiments have been performed at room temperature on high-quality epitaxially grown Y-Ba-Cu-O(001) single-crystal thin films, showing the sharp (1×1) LEED patterns, to explore the normal-state electronic structure. We found some evidence for the existence of a clear Fermi edge and the k-space dispersion of the photoemission features, which are contrary to what is naively expected from the previous belief that the electronic structure of this oxide is highly localized and correlated. We presented the experimental valence-band structure $E(k)$ of Y-Ba-Cu-O over the whole Brillouin zone, which seems to be consistent, though not quantitative agreement, with some of the calculated band structures previously reported. Note that our results do not necessarily tend to prove the existing band-structure calculations for Y-Ba-Cu-O and to confirm the traditional BCS mechanism, however. *It may be fair to say that whether or not the band concept is valid in this oxide should be reconsidered prudently.* One should not trust a conclusion unless accurate data on high-quality samples are presented.

Finally, we want to assess briefly the AIUPS findings[4–15] which were regarded as conclusive evidence of the importance of electron correlation effects and the breakdown of the one-electron picture in this oxide. These findings are (i) no observation of a clear Fermi edge, (ii) the almost uniform shift of the measured density of states to higher binding energy with respect to the theoretical one by ~ 1–2 eV, and (iii) the appearance of a Cu $3d^8$ final-state satellite in the valence band [see also Fig. 2(b)]. First, as for (i), we have shown the existence of a clear Fermi edge (see also Ref. 28). Second, as has been states in Sec. I, electron correlations are strong in any metal. A discrepancy between theory and experiment as to the absolute binding energies of the different valence bands is not a new finding. Such a discrepancy of ~ 1 eV (or 20%–30%) has also been observed in transition metals[30,41,42] and even in simple metals.[43,44] Third, as for (iii), we note that whether or not a valence-band satellite exists cannot judge the importance of electron correlations. For example, such a satellite was never discovered in Cr (Ref. 30) and Fe (Ref. 45), though it was done in Ni (Ref. 42) and Cu.[46] In Cu and Y-Ba-Cu-O, no satellite is clearly observed except near the Cu $3p$ resonance. The Coulomb intra-atomic energy U_{dd} between d electrons has been estimated to be ~ 6 eV in the past by using a cluster model with many parameters and adjusting the parameters to get the best fit to the observed spectra[6,7] and by using the simple relation $E_s=2E_d+U_{dd}$, where E_s is the binding energy of the satellite and E_d the binding energy of the main d band. A cluster model is a reasonable zero-order approximation for systems in which U_{dd} is expected to be very large and bandwidth is neglected and, therefore, may naturally lead to the large U_{dd} value. Let us notice that the U_{dd} obtained in these models is not the energy U of charge fluctuations, $d^n+d^n\rightarrow d^{n+1}+d^{n-1}$ (or $d^ns+d^ns\rightarrow d^{n+1}+d^{n-1}s^2$), of the Hubbard model. They may not be identical even in the atomic limit. The previous studies of the valence-band satellite in Ni showed that the band model is a reasonable approximation for the ground state and the electron correlations can be treated within perturbation theory.[47–50] Furthermore, it has been shown that it is not easy to deduce U_{dd} from experimental data. In conclusion, the AIUPS findings (i)–(iii) are insufficient to conclude the band picture to be broken down in this oxide.

ACKNOWLEDGMENTS

We are pleased to thank the staff of the Photon Factory, National Laboratory for High Energy Physics, for their excellent support. This work has been performed under the approval of the Photon Factory Program Advisory Committee (Proposal No. 88-U-002).

[1]M. K. Wu, J. R. Ashburn, C. J. Torng, P. H. Hor, R. L. Meng, L. Gao, Z. J. Huang, Y. Q. Wang, and C. W. Chu, Phys. Rev. Lett. **58**, 908 (1987).

[2]J. Bardeen, L. N. Cooper, and J. R. Schrieffer, Phys. Rev. **106**, 162 (1957); **108**, 1175 (1957).

[3]B. Batlogg, R. J. Cava, A. Jayaraman, R. B. van Dover, G. A. Kourouklis, S. Sunshine, D. W. Murphy, L. W. Rupp, H. S. Chen, A. White, K. T. Short, A. M. Mujsce, and E. A. Rietman, Phys. Rev. Lett. **58**, 2333 (1987).

[4]P. D. Johnson, S. L. Qiu, L. Jiang, M. W. Ruckman, M. Strongin, S. L. Hulbert, R. F. Garrett, B. Sinkovic, N. V. Smith, R. J. Cava, C. S. Jee, D. Nichols, E. Kaczanowicz, R. E. Salomon, and J. E. Crow, Phys. Rev. B **35**, 8811 (1987).

[5]R. L. Kurtz, R. L. Stockbauer, D. Mueller, A. Shih, L. E. Toth, M. Osofsky, and S. A. Wolf, Phys. Rev. B **35**, 8818 (1987).

[6]A. Fujimori, E. Takayama-Muromachi, Y. Uchida, and B. Okai, Phys. Rev. B **35**, 8814 (1987).

[7]A. Fujimori, E. Takayama-Muromachi, and Y. Uchida, Solid State Commun. **63**, 857 (1987).

[8]M. Onellion, Y. Chang, D. W. Niles, R. Joynt, G. Margaritondo, N. G. Stoffel, and J. M. Tarascon, Phys. Rev. B **36**, 819 (1987).

[9]J. A. Yarmoff, D. R. Clarke, W. Drube, U. O. Karlsson, A. Taleb-Ibrahimi, and F. J. Himpsel, Phys. Rev. B **36**, 3967 (1987).

[10]N. G. Stoffel, J. M. Tarascon, Y. Chang, M. Onellion, D. W. Niles, and G. Margaritondo, Phys. Rev. B **36**, 3986 (1987).

[11]E. R. Moog, S. D. Bader, A. J. Arko, and B. K. Flandermeyer, Phys. Rev. B **36**, 5583 (1987).

[12]T. Takahashi, F. Maeda, H. Arai, H. Katayama-Yoshida, Y. Okabe, T. Suzuki, S. Hosoya, A. Fujimori, T. Shidara, T. Koide, T. Miyahara, M. Onoda, S. Shamoto, and M. Sato, Phys. Rev. B **36**, 5686 (1987).

[13]Z. Shen, J. W. Allen, J. J. Yeh, J. S. Kang, W. Ellis, W. Spicer, I. Lindau, M. B. Maple, Y. D. Dalichaouch, M. S. Torikachvili, J. Z. Sun, and T. H. Geballe, Phys. Rev. B **36**, 8414 (1987).

[14]S. L. Qiu, M. W. Ruckman, N. B. Brookes, P. D. Johnson, J. Chen, C. L. Lin, M. Strongin, B. Sinkovic, J. E. Crow, and C. Jee, Phys. Rev. B **37**, 3747 (1988).

[15]A. Samasvar, T. Miller, T. C. Chiang, B. G. Pazol, T. A. Friedmann, and D. M. Ginsberg, Phys. Rev. B **37**, 5164 (1988).

[16]L. F. Mattheiss and D. R. Hamann, Solid State Commun. **63**, 395 (1987).

[17]S. Massidda, J. Yu, A. J. Freeman, and D. D. Koelling, Phys. Lett. A **122**, 198 (1987).

[18]J. Yu, S. Massidda, A. J. Freeman, and D. D. Koelling, Phys. Lett. A **122**, 203 (1987).

[19]G. Zhao, Y. Xu, W. Y. Ching, and K. W. Wong, Phys. Rev. B **36**, 7203 (1987).

[20]B. Szpunar and V. H. Smith, Phys. Rev. B **37**, 7525 (1988).

[21]B. A. Richert and R. E. Allen, Phys. Rev. B **37**, 7869 (1988).

[22]Y. Xu, W. Y. Ching, and K. W. Wong, Phys. Rev. B **37**, 9773 (1988).

[23]F. P. Bowden and D. Tabor, *The Friction and Lubrication of Solids* (Oxford Univ. Press, London, 1956); M. Fink and D. Hofman, Z. Metallkd. **3**, 24 (1932).

[24]R. A. Rosenberg and C. R. Wen, Phys. Rev. B **37**, 5841 (1988); **37**, 9852 (1988).

[25]N. Nucker, J. Fink, J. C. Fuggle, P. J. Durham, and W. M. Temmerman, Phys. Rev. B **37**, 5158 (1988).

[26]N. G. Stoffel, P. A. Morris, W. A. Bonner, D. LaGraffe, M. Tang, Y. Chang, G. Margaritondo, and M. Onellion, Phys. Rev. B **38**, 213 (1988).

[27]N. G. Stoffel, Y. Chang, M. K. Kelly, L. Dottl, M. Onellion, P. A. Morris, W. A. Bonner, and G. Margaritondo, Phys. Rev. B **37**, 7952 (1988). Note that their samples had the very wide transition width $\Delta T(10\%-90\%)$ of ~ 40 K. They found no fine structures near E_F but only long tails.

[28]L. Hoffmann, A. A. Manuel, M. Peter, E. Walker, and M. A. Damento, Physica C **153–155**, 129 (1988).

[29]Y. Sakisaka, T. Komeda, T. Maruyama, M. Onchi, H. Kato, Y. Aiura, H. Yanashima, T. Terashima, Y. Bando, K. Iijima, K. Yamamoto, and K. Hirata, Phys. Rev. B **39**, 2304 (1989).

[30]Y. Sakisaka, T. Komeda, M. Onchi, H. Kato, S. Suzuki, K. Edamoto, and Y. Aiura, Phys. Rev. B **38**, 1131 (1988), and references therein.

[31]Preliminary studies showed that oxygen starts to leave our samples when heating in vacuum at above $\sim 150\,^{\circ}$C.

[32]T. Terashima, K. Iijima, K. Yamamoto, Y. Bando, and H. Mazaki, Jpn. J. Appl. Phys. **27**, L91 (1988).

[33]C. Benndorf, B. Egert, G. Keller, H. Seidel, and F. Thieme, J. Phys. Chem. Solids **40**, 877 (1979).

[34]N. G. Stoffel, P. A. Morris, W. A. Bonner, D. LaGraffe, M. Tang, Y. Chang, G. Margaritondo, and M. Onellion, Phys. Rev. B **38**, 213 (1988).

[35]M. Tang, N. G. Stoffel, Q. B. Chen, D. LaGraffe, P. A. Morris, W. A. Bonner, G. Margaritondo, and M. Onellion, Phys. Rev. B **38**, 897 (1988).

[36]G. Wendin, J. Phys. (Paris) Colloq. **48**, C9-1157 (1987). Note that G. Wendin himself has ruled out such an interpretation in terms of an O $2p^4$ two-hole satellite, however (private communication).

[37]J. J. Yeh and I. Lindau, At. Data Nucl. Tables **32**, 1 (1985).

[38]The existence of a Fermi surface means that each one-electron level can be described rigorously by a well-defined wave vector **k**, a good quantum number, in k space.

[39]The noise level and the total energy resolution of 0.15 eV at $h\nu=40$ eV and 0.1 eV at $h\nu=23$ eV are small enough to observe such fine structures, the lifetime broadening effects of which are very small in the Fermi-edge region (Landau's Fermi-liquid theory).

[40]W. K. Ford, C. T. Chen, J. Anderson, J. Kwo, S. H. Liou, M. Hong, G. V. Rubenacker, and J. E. Drumheller, Phys. Rev. B **37**, 7924 (1988).

[41]Y. Sakisaka, T. Rhodin, and D. Mueller, Solid State Commun. **53**, 793 (1985), and references therein.

[42]Y. Sakisaka, T. Komeda, M. Onchi, H. Kato, S. Masuda, and K. Yagi, Phys. Rev. Lett. **58**, 733 (1987); Phys. Rev. B **36**,

6383 (1987), and references therein.
[43]R. A. Bartynski, R. H. Gaylord, T. Gustafsson, and E. W. Plummer, Phys. Rev. B **33**, 3644 (1986).
[44]I.-W. Lyo and E. W. Plummer, Phys. Rev. Lett. **60**, 1558 (1988).
[45]H. Kato, T. Ishii, S. Masuda, Y. Harada, T. Miyano, T. Komeda, M. Onchi, and Y. Sakisaka, Phys. Rev. B **32**, 1992 (1985); **34**, 8973 (1986).
[46]M. Iwan, F. J. Himpsel, and D. E. Eastman, Phys. Rev. Lett. **43**, 1829 (1979).
[47]D. R. Penn, Phys. Rev. Lett. **42**, 921 (1979).
[48]A. Liebsch, Phys. Rev. Lett. **43**, 1431 (1979).
[49]L. C. Davis and L. A. Feldkamp, Solid State Commun. **34**, 141 (1980).
[50]G. Treglia, F. Ducastelle, and D. Spanjaard, J. Phys. (Paris) **43**, 341 (1982).

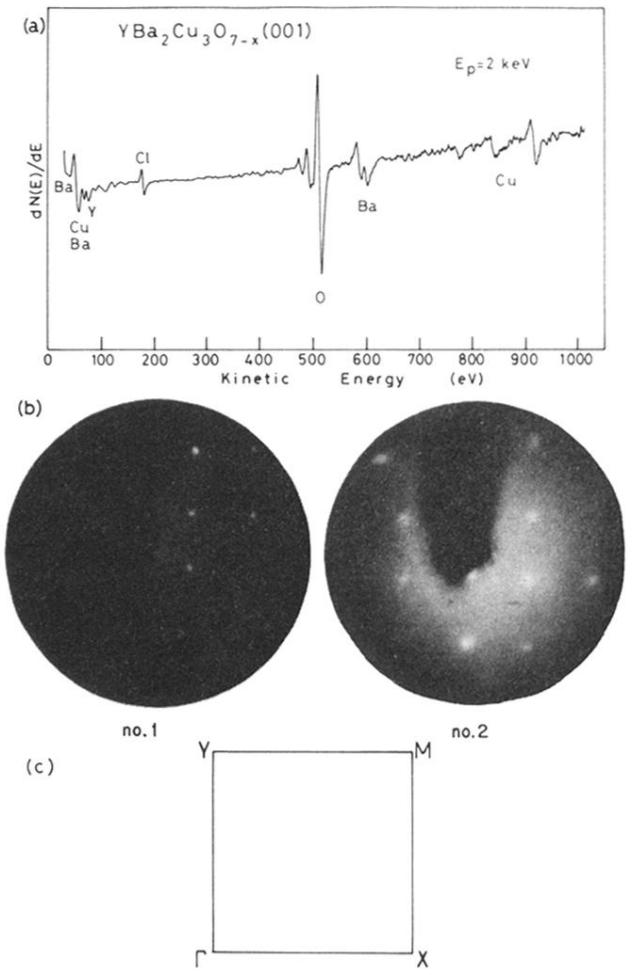

FIG. 1. (a) Typical Auger spectrum of $YBa_2Cu_3O_{7-x}$ (001) ($E_p = 2$ keV). (b) LEED patterns for $YBa_2Cu_3O_{7-x}$ (001), No. 1 ($E_p = 74$ eV) [left] and No. 2 ($E_p = 68$ eV) [right]. (c) ΓXMY[(001)] plane of the Brillouin zone.